The Box-Counting Fractal Dimension: Does it Provide an Accurate Subsidy for Experimental Shape Characterization? If So, How to Use It?

REGINA CÉLIA COELHO[1]
LUCIANO DA FONTOURA COSTA[1]

[1]Cybernetic Vision Research Group
IFSC - University of São Paulo
Caixa Postal 369, São Carlos, SP, 13560, Brazil
FAX: +55 (162) 71 3616
reginac@ifqsc.sc.usp.br
luciano@ifqsc.sc.usp.br

Abstract. This paper reports an experimental assessment of how appropriate and accurate the self-similarity or box-counting fractal dimension is for practical applications to the analysis and characterization of natural objects. The effects of the partial fractality of real objects as well as the limited representation allowed by typical spatially quantized images are investigated through a series of experimental measurements respectively to two Koch curves. Practical guidelines are established and discussed that can help in obtaining more precise and meaningful experimental results. These guidelines are illustrated with respect to images of synthetic neural cells.

1. Introduction

Fractal geometry provides an elegant framework that can be taken as basis for theoretically analysing and characterizing complex curves exhibiting some kind of intrinsic self-similarity at different magnification scales [Mandelbrot (1983), Peitgen-Saupe (1988), Falconer (1990), Edgar (1990), Gleick (1990)]. Contrariwise to traditional Euclidian geometry, which deals with smooth curves presenting continuous derivatives and which tend to straight lines as the magnification scale is increased, fractal elements are characterized by irregularity within a range of distinct magnification scales. Fractal elements such as Koch's curves involve the recursive repetition *ad infinitum* of an elementary geometric pattern, in such a way that parts of the curve appear similar whatever the scale in which they are observed. The self-similarity (also known as box-counting or Bouligand-Minkowski, or simply Minkowski) dimension [Peitgen-Saupe (1988), Falconer (1990)], henceforth abbreviated as D, provides a measure of the degree of 'space-filling' exhibited by a particular fractal curve. In two-dimensional spaces, D can take any value inside the interval [1,2]. Low values of D indicate that the fractal curves tend to a traditional curve with topological dimension of 1; high values of D indicate that the fractal curve tends to the two-dimensional surface. The fractal dimension presents fundamental importance in fractal geometry, as well as many practical applications. It should be observed that the box-counting dimension is not the same as the Hausdorff dimension [Falconer (1990)].

Over the last decade, the box-counting dimension has been increasingly applied as a means of characterizing the shape of a series of natural objects, from neurons to clouds. One of the recent applications of the box-counting dimension has been to the characterization of space coverage by dendritical and axonal arborizations of neural cells [Montague-Friedlander (1989), Montague-Friedlander (1991)], which is of special interest regarding the current research activities being pursued by us at the Cybernetic Vision Research Group, IFSC-USP, thus motivating the work reported in this paper. More specifically, we have been concerned about how much the accuracy of the box-counting dimension is distorted by the following two issues: (a) natural objects, such as a neuron, are not fractal at all the possible magnification scales, a property that will be henceforth denominated *limited (or partial) fractality*, and (b) the discrete nature of the images in which such features are usually represented limits the accuracy for the estimation of D.

This paper presents an experimental assessment of the accuracy of the box-counting approach. The effects of limited fractality and the spatial quantization imposed by typical computer

images are discussed from the perspective of obtained measurements with respect to two Koch curves, whose theoretical self-similarity fractal dimensions are precisely known. The obtained results are discussed and taken as basis to define some practical guidelines that can contribute to more accurate experimental estimations of D. Such results are then applied respectively to the characterization of synthetic neural cells generated by a stochastic vectorial grammar [Coelho-Costa (1994)]. The principal contributions of the present paper consists in: (i) the indication that, unlike it has been so often adopted in the literature, extreme care should be taken while experimentally estimating and interpreting the box-counting dimension, and (ii) some practical results and guidelines allowing such a more careful assessment are presented and exemplified respectively to the characterization of neural cells.

2. The Box-Counting Dimension and Koch Curves

Let us illustrate the concept and interpretation of D in terms of the broadly known Koch curves. Such curves are best described from the perspective of their recursive construction, which is characterized by the replacement of each of the straight line segments at a given generating stage by a basic geometric pattern henceforth to be called the *generating pattern*. Figure 1 illustrates two Koch curves that are respectively produced by the recursive replacement construction [Mandelbrot (1977), Stevens (1989), Peitgen-Saupe (1988), Edgar (1990)].

Instead of a single line segment, the initial shape can alternatively be a triangle, a square, or any other polygon. It is henceforth assumed that, at the generating stage n=0, the polygons have S sides, each possessing length $\delta(0)$, thus adding up to the total perimeter of $P(0)=S.\delta(0)$. It is also assumed that the generating pattern is composed by N segments with relative lengths $r = \delta(n)/T(n) = \text{constant}$, where $\delta(n)$ and T(n) are, respectively, the absolute length of each segment and the distance between the initial and final point of the generating pattern at the n-th generation stage (n=1,2,...). Under these circumstances, the box-counting dimension is given as $D=\text{Log}(N)/\text{Log}(1/r)$ [Peitgen (1988), Falconer (1990), Stevens (1989)], which leads to $D_1=\text{Log}(4)/\text{Log}(3)$ and $D_2=\text{Log}(8)/\text{Log}(4)=1.5$ respectively to the Koch curves depicted in Figure 1(a) and (b). The higher value obtained for the Koch curve represented in Figure 1(b) expresses the fact that it provides a relatively higher degree of 'space-filling'.

In addition, it is straightforward to verify that $\delta(n)=r.\ \delta(n-1)=r^n.\ \delta(0)$, that the amount of line segments at the n-th stage is $A(n)=N^n.S$, and that, consequently, $P(n)=A(n).\delta(n)=N^n.S.r^n.\delta(0)=(N.r)^n.P(0)$. It follows directly that when $n\rightarrow\infty$ the perimeter will also be infinite.

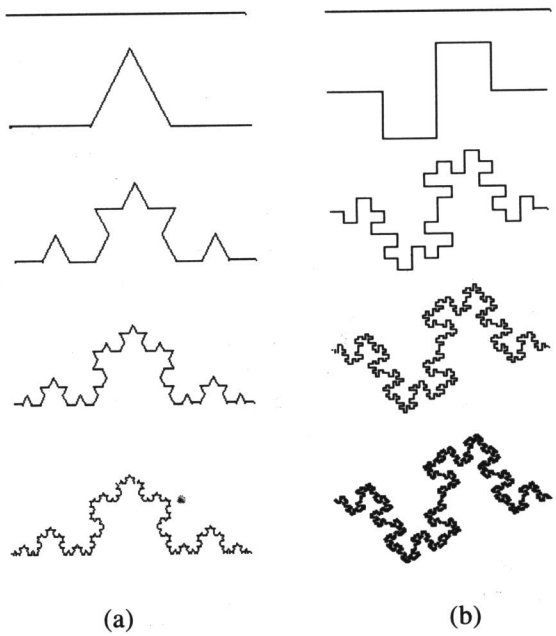

(a) (b)

Figure 1 - Two Koch curves.

The counting box technique [Falconer (1990), Feder (1988), Montague-Friedlander (1989), Montague-Friedlander (1991)] is one of the most commonly adopted approaches for the experimental characterization of the fractal nature of objects. Its basic processing step consists in projecting the shape to be investigated onto a regular orthogonal grid, with cells (i.e. 'boxes') of size *dxd*, and counting the number *N(d)* of cells that happen to contain part of the projected shape. Such a procedure is repeated for a series of different values of *d* and it can be verified that the absolute value of the slope of the least mean square (or eigenvalue/eigenvector) fitting applied to the set of sampled values *{Log(d), Log(N(d))}* provides an approximation of D. As observed in the previous section, this approximation will however suffer the effects caused by image quantization and the partial fractality exhibited by natural objects. As far as this latter effect is concerned, some insight can be gained about how it affects the box-counting dimension estimation of shapes exhibiting partial fractality by means of some theoretical reasoning. Let us assume that a specific Koch curve was produced only up to the

maximum generating stage N. The obtained Koch curve will thus be composed by straight line segments with length $\delta(N)= r^N\delta(0)$. As *d* becomes smaller, it will reach a stage where it gets smaller than $\delta(N)$ and, from this point on, the curve will no longer be measured as a fractal, but rather as a conventional curve with D=1. It is thus clear that the curve *Log(N(d))x Log(d)* will typically include two distinct regions: one in which the fractal nature of the shape is dominant (D>1) and the other where the $\delta(N)$ has become larger than *d* (D=1). The overall shape of such a predicted overall shape for the curve *Log(N(d))xLog(d)* is presented in Figure 2. Although the point P has been indicated as dividing the two parts of the curve, it should be observed that the transition from one region to the other will not be so abrupt and that an intermediate region will be obtained. Figure 2 also presents the convention for W and S that is adopted in the next Section.

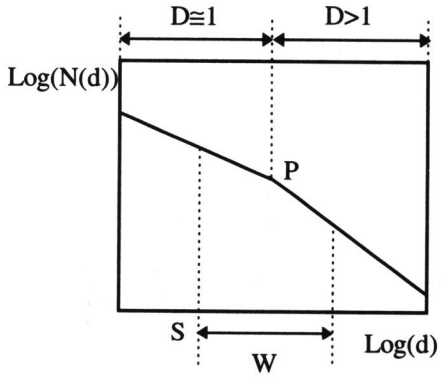

Figure 2 - The overall shape of the curve *Log(N(d))x Log(d)* with respect to a partially fractal shape.

In spite of all the potential of the discrete nature of the image and the partial fractality of real shapes for disrupting the estimation of the fractal dimension, little attention has been paid to such important issues. In practice, the majority of experimental works reported in the literature have been limited to estimating *N(d)* for a series of *d* and processing linear regression over the whole curve *Log(N(d))x Log(d).* The next section presents an experimental assessment of the counting-boxes strategy respectively to the two Koch curves showed in Figure 1, as well as some guidelines that can be applied in order to obtain more precise estimation of D.

3. Experimental Results

This section presents a series of experimental investigations aimed at characterizing the suitability of the box-counting dimension as a practical means for shape characterization and analysis. The underlying approach has been to apply the counting-boxes algorithm over the two Koch curves presented in Figure 1, whose ideal continuous representations have theoretical fractal dimensions known to be equal to *Log(4)/Log(3)* and 1.5 respectively. The Koch curves were obtained by using an algorithm for straight line segment generation which produces straight features obeying the grid-intersect quantization scheme [Stevens (1989), Freeman (1974)]. The obtained results are presented and discussed in the following subsections.

3.1. Influence of the Limited Resolution Implied by the Image Spatial Quantization

As the generating stage of the Koch curves increases, the new details added to the overall fractal curve become smaller and smaller. When the spatial sampling limit resolution in which the image is being generated is reached, the added features will no longer be representable and the overall curve will cease to grow.

This suggests a test can be devised to express the degradation implied by the finite spatial sampling resolution onto the representation of fractal objects. Such a test consists in calculating the difference D_i between the images representing the fractal curves at the generating stages *i* and *i-1*, *i=0,1,2,...* (*i=-1* correspond to a single pixel) This difference expresses the number pixels that appear at a given generating stage and do not appear in the subsequent stage and vice-versa. It can be verified that D_i follow the recursive relation $D_i= (4/3)^{i-1}D_{i-1}$, with respect to the Koch curves in Figure 1(a). Such theoretical results (curve A), together with the respective experimental results (curve B), are showed in Figures 3(a), (b) and (c) respectively to $\delta(0)$=50, 100 and 200. Similar results for the Koch curve in Figure 1(b) are depicted in Figures 4(a), (b) and (c), where the theoretical values of D_i (curve B) are know to obey the the recursive relation $D_i=2. D_{i-1}$.

By comparing the theoretical with the experimental results in Figures 3 and 4, it can be easily verified that the values of these latter start to collapse after reaching a critical value of *i*, thus indicating that

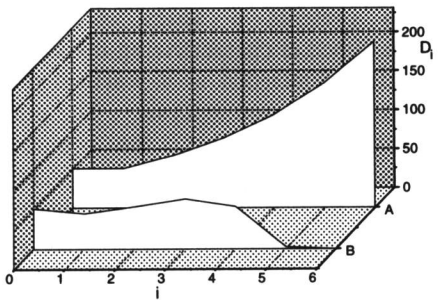

(a)

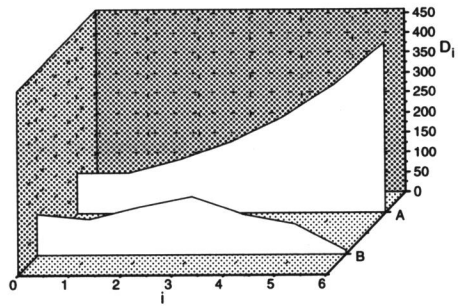

(b)

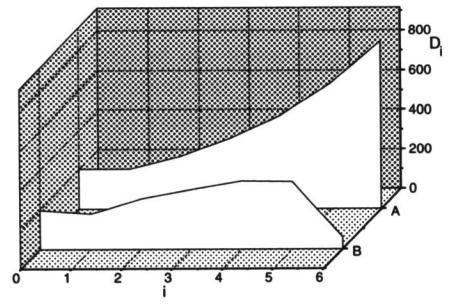

(c)

Figure 3 - Differences between generate of stage for the Koch curves in Figure 1(a).

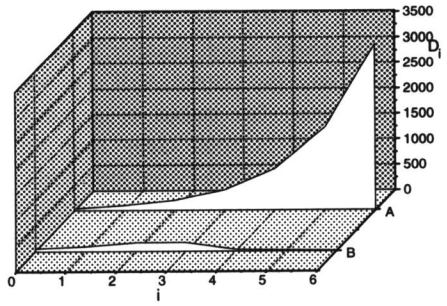

(a)

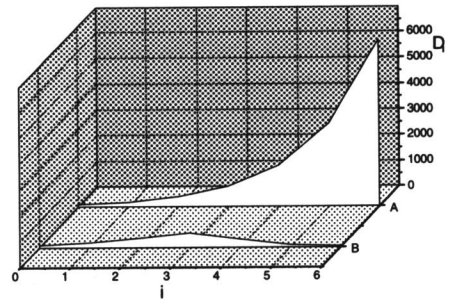

(b)

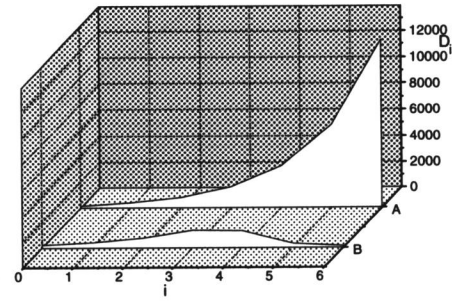

(c)

Figure 4 - Differences between generate of stages for the Koch curves in Figure 1(b).

the new added details will no longer be properly represented starting from the generating stage *i*. As it could be expected, the critical point is reached earlier for smaller $\delta(0)$ in both curves. For the Koch curve in Figure 1(a), only 3 generating stages are properly processed for $\delta(0)=50$, which is extended to 4 stages in the case of $\delta(0)=100$ and 200. The second Koch curve starts to deteriorate after 3 generation stages for $\delta(0)=50$ and 100 and 4 stages for $\delta(0)=200$. it can be verified that the critical value of *i* is associated to the stage where the straight line segments constituting the generating pattern reaches the dimension of a pixel in the image.

3.2. The Influence of the Partial Fractality

In addition to the limit imposed by the discrete nature of the image space, natural objects often present an inherent limited fractality. The dendritical arborizations of neural cells, for instance, have its fractal characteristics limited by the finite orders of

dendritic branches. In order to investigate how such a property can influence the estimation of D, a series of images containing Koch curves generated up to the maximum the generating stage N=0,1,2,3, and 4 were processed in order to obtain the diagrams of *Log(N(d))* in terms of *Log(d)* that are depicted in Figures 5 and 6. A straight line (dashed) with slope of -1 was also added to the plots in order to provide a reference for visual comparison. As it was expected, the curves for N=0, which correspond to typical straight lines, presents a strong similarity with the reference curve possessing slope of -1. It should be observed that the experimental curves becomes more and more noisy as *Log(d)* is increased. Such an effect is caused by a combination of the finite extent of the generated Koch curves and the spatially quantized nature of the image space. It can be also verified that, as N_{max} increases, the curves tend to become more and more inclined, i.e. the value of the absolute value of their respective overall slope increases, thus surpassing the topological dimension. This effect is more evident for the curves in Figure 6, which were obtained.

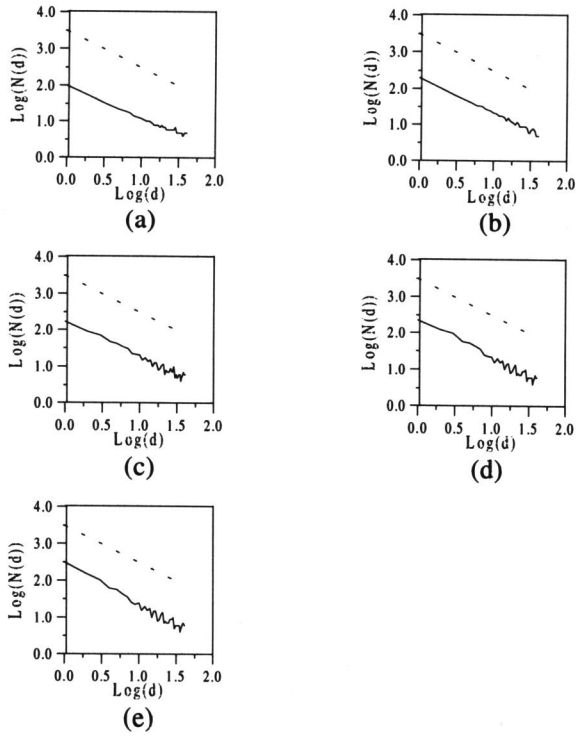

Figure 5 - Curves Log(N(d))xLog(d) for the Koch curve in Figure 1(a).

As it would be expected, the obtained curve converges to a standard curve with D=1 for N=0 (i.e. a single line is represented in the image). The two regions discussed in the previous section (D≅1 and D>1) can be identified with the aid of a ruler in many of the graphs in Figure 5 and 6.

The relative errors (in %) of the estimated D in terms of the position *S* (see Figure 2) assumed for the linear regression for W=10, 20 and 30 are presented in Figures 7 and 8 respectively to the Koch curves in Figures 1(a) and (b). One of the first interesting features to be observed in such graphs regards the reduction of the overall estimation error (i.e. the average value of the curves along the domain S) caused by the increase of the fractality (i.e. larger N) of the respective Koch curves. It can be readily verified that rather noisy results were obtained at the right portion of the plots for W=10, which reflect the fact that the narrow window too sensitive to the noisy portions (Figures 5 and 6). The effectiveness of larger values of W as a means of 'smoothing' the obtained curves is clearly verified. However, larger values of W also imply a higher average value of the obtained errors. The effect of S over the error is also substantial. As N increases, the value of S for which the error is minimum tend to shift to the right.

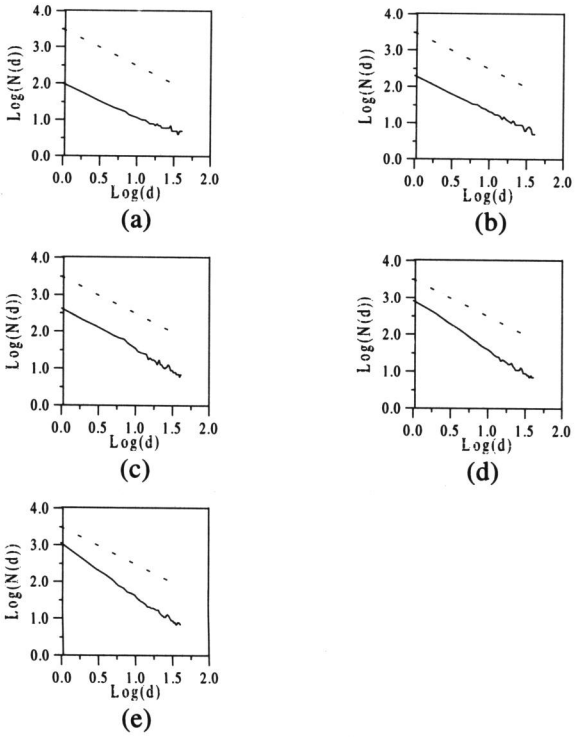

Figure 6 - Curves Log(N(d))xLog(d) for the Koch curve in Figure 1(b).

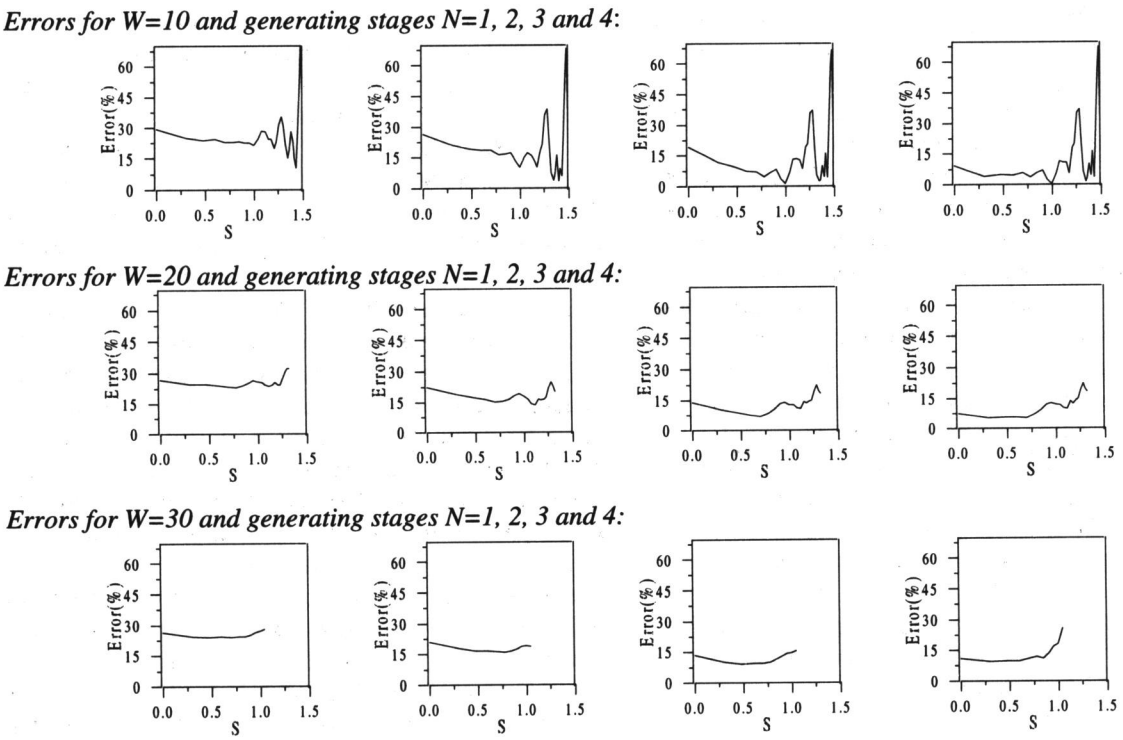

Figure 7 - Errors (in %) respectively to the Koch curve in Figure 1(a).

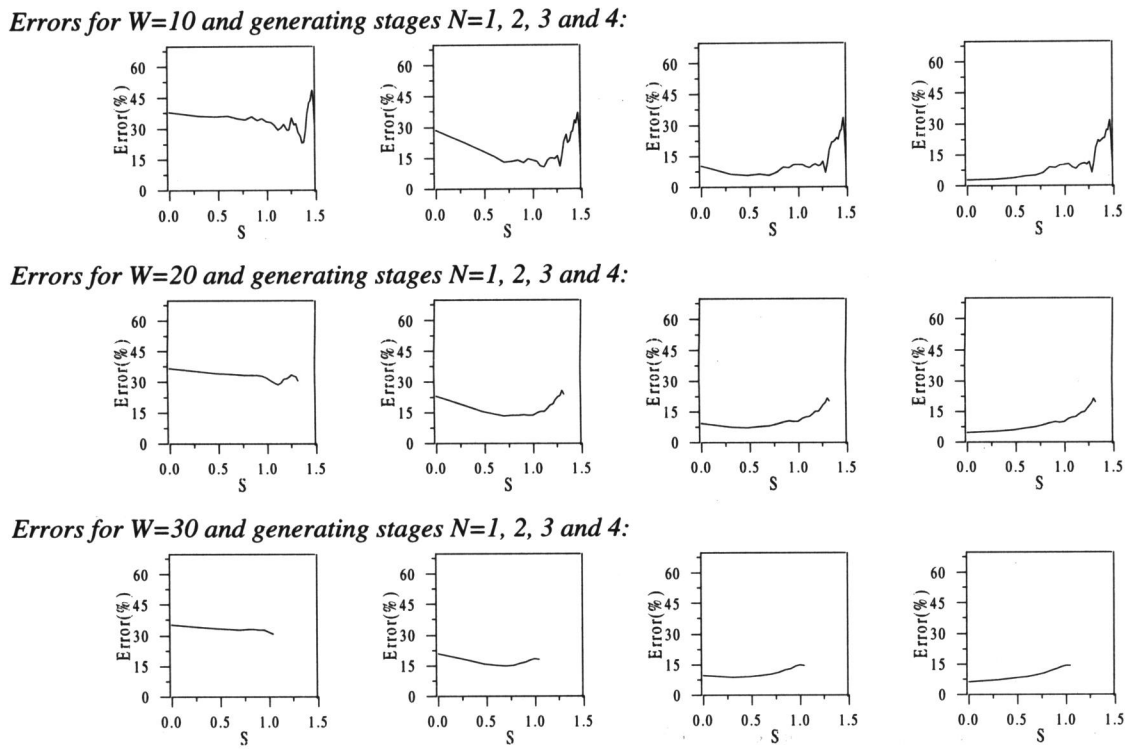

Figure 8 - Errors (in %) respectively to the Koch curve in Figure 1(b).

3.3. Practical Guidelines for Improving the Experimental Estimation of D

As indicated by the above presented results, it is clear that D can vary wildly according to the region overwhich the linear regression needed for the estimation of D is performed. It can be verified that the most important issue behind the accurate estimation of D consists in identifying the appropriate range of values of *d* to be used during the linear regression. As verified in the previous sections, this window should be defined in terms of the region where the curve exhibit fractal features and be limited by the resolution of the spatial quantization in the image. While the latter constraint can be reasonably well defined by adopting the minimum value of d to be larger than $\delta(N)$ (i.e. size in pixels of the smallest segments in the image), the problem of identifying an appropriate region where the object is fractal is not straightforward to be accomplished. Moreover, as indicated in Figures 5 to 8, the fractal region tends to correspond to large values of *d*, where the experimentally derived values of *Log(N(d))* are most noisy. The choice of the appropriate region, i.e. the selection of S and W, can be done with basis on the graphical representation of the curve *Log(N(d))xLog(d)* by identifying the region where $D \cong 1$, which always extend from $d=1$. This can be done visually by using a ruler, in such a means that the point where the curve breaks from this region is taken as a good value for S. The value of W can then be set as equal to the extent from S to the point where the curve *Log(N(d))xLog(d)* becomes too noisy. This technique has been verified to lead to good results, including the situations depicted in Figures 5 and 6. Let us consider, for instance, Figure 6(c). It is easily verified that S should be selected as approximately $S=10^{0.7}=5$ and that $W=10^{1.4} - 10^{0.7}=20$, which lead to an error smaller than 10%.

4. Application to the Morphometric Characterization of Neural Cells

In this section, the above proposed guidelines are illustrated with respect to images of synthesized neural cells, presented in Figure 9(a) and (b), which exhibit fractality arising from the recursive patterns of dendritical branching, which is obviously limited. The *Log(N(d))xLog(d)* curves obtained for such objects are presented in Figure 10(a) and (b), respectively. By using the proposed guidelines, the values of $D_a=1.384$ and $D_b=1.476$ were obtained with respect to the neural cells in Figures 9(a) and (b). The fact that $D_a<D_b$ reflects the higher 'space filling' characteristic exhibited by the neural cell in Figure 7(b). It is interesting to notice that, were the suggested guidelines not applied, the obtained values of D could have been resulted much smaller.

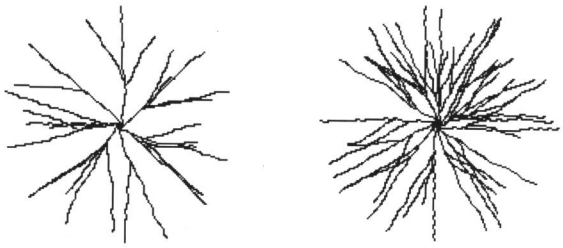

(a) (b)

Figure 9 - Neural cells.

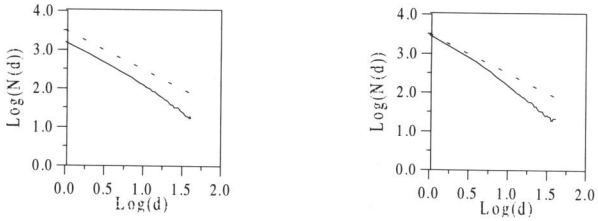

(a) (b)

Figure 10 - Curves Log(N(d))xLog(d) for the neurons in Figures 9(a) and (b).

5. Concluding Remarks

This paper has addressed the problem of accurate estimation of the Minkowski dimension through the box-counting algorithm that has been so often applied as a means of shape characterization and analysis. It has been verified and discussed that two major effects contributes to producing distorted values of D, namely the finite spatial resolution allowed by computer images and the limited fractality of real objects. The assessment of the box-counting approach, performed respectively to two Koch curves for which the theoretical Ds are precisely known, substantiated that wildly varying results can be obtained if extreme care is not taken. Such an experimental assessment indicated that the limited spatial resolution of real computer images severely constraints the fidelity in which fractal elements can be represented. For objects possessing width of about 100 pixels, no more than 3 or 4 fractal generating order will be properly represented. It was also verified that the *Log(N(d))xLog(d)* curve typically presents two

constituent regions, one in which D≅1 (topological section) that is followed by another region in which D>1 (fractal section). The errors for the estimation of D In terms of S, W and the object fractality were investigated and a series of results were obtained. Firstly, it was verified that the fractality of the produced Koch curves affect directly the average value of the error. It was also verified that the regions where *d* is large are typically characterized by noise caused by the finite extent of the Koch curves and the discrete nature of the image space. The value of W was verified to provide an effective means for smoothing such noise. In brief, it was clearly verified that, unless great care is taken for selecting the region where the least mean square fitting is applied, large errors will be obtained. Practical guidelines were proposed as a means of improving the accuracy for the estimation of D, which were verified to produce good results. Such guidelines were illustrate with respect to two synthetically generated neural cells.

Although the proposed technique has yielded good results, it depends on an operator-assisted choice of S and W, which can imply some subjectiveness to the overall process. Efforts are currently being made towards developing a fully automated process for the accurate estimation of D, and a novel multi-scale approach to accurate curvature estimation is being considered as a means of characterizing the curve *Log(N(d))xLog(d)* and providing an accurate choice of S and W. Such developments should also include averaging for several positions and orientations of the grid.

Acknowledgments

Luciano da F. Costa is grateful to FAPESP (Proc. 94/3536-6) and CNPq (Proc. 301422/92-13) for financial support.

Bibliography

G. A. Edgar, *Measure, Topology, and Fractal Geometry.* Spring-Verlag New York Inc., 1990.

R. C. Coelho, L. da F. Costa, Gramáticas para Sínteses de Estruturas Neurais, *Anais do Workshop sobre Visão Cibernética* (1994) 74-79.

K. Falcolner, *Fractal Geometry-Mathematical Foundations and Applications.* Jhon Wiley & Sons Ltd., England, 1990.

J. Feder, *Fractals.* Plenum Press, 1988.

H. Freeman, Computer Processing of Line-drawing images. *Computing Surveys* **6** No. 1 (1974) 57-97.

J. Gleick, *CAOS - A Criação de uma Nova Ciência.* Editora Campus, 1990.

B. B. Mandelbrot, *The Fractal Geometry of Nature.* W. H. Freeman and Company, 1977.

P. R. Montague, M. J. Friedlander, Expression of an Intrinsic Growth Strategy by Mammalian Retinal Neurons. *Neurobiology* **86** (1989) 7223-7227.

P. R. Montague, M. J. Friedlander, Morphogenesis and Territorial Coverage by Isolated Mammalian Retinal Ganglion Cells. *The Journal of Neuroscience* **11** No. 5 (1991) 1440-1457.

H. -0. Peitgen, D. Saupe, *The Science of fractal Images.* Springer-Verlag New York Inc., 1988.

R. T. Stevens, *Fractal Programming in C.* M&T Publishing Inc., 1989.